Papers

Dynamic Stark Effect in CH_3F and Other Optically Pumped Lasers

T. Y. CHANG, MEMBER, IEEE

Abstract—The dynamic Stark effect in optically pumped lasers is discussed. Javan's theory of three-level masers is extended and elucidated by transforming his expressions into new forms in which all of the major terms can be deduced from a modified energy-level diagram through simple physical arguments. The gain spectra of high-power 496-μm CH_3F lasers are calculated from the theory. Contrary to previous interpretations, the wide emission bandwidth at pump intensities above 30 kW/cm^2 is shown to be primarily due to the dynamic Stark effect on $K = 1$, 2, and 3 components. It is found that to obtain a narrow emission bandwidth the pump intensity should be kept below 10 kW/cm^2.

I. Introduction

THE dynamic (or ac) Stark effect is a phenomenon that arises whenever an atomic or molecular electric-dipole transition (henceforth referred to as the pump transition) is subjected to perturbation by a strong, near-resonant, monochromatic radiation field. The effect manifests itself as the splitting and shifting of a coupled electric-dipole transition (henceforth referred to as the probe transition) connecting one of the perturbed energy levels with a third energy level. Since the pioneering work of Autler and Townes in 1955 [1], who used rotational levels in OCS for their investigation, experimental studies of the effect have been extended to electronic levels using either two-photon absorption [2] or stimulated emission [3], and to vibrational-rotational levels using stimulated emission [4]. The purpose of this paper is 1) to elucidate the theory of dynamic Stark effect for optically pumped lasers involving only collision broadened transitions, and 2) to present a numerical study for the case of high-power CH_3F far infrared (FIR) lasers. A theory developed by Javan [6] for this kind of system is the basis of our discussion. Although the expressions obtained by Javan are useful for numerical calculations of dynamic Stark spectra, they are unfortunately too complex in form to provide a qualitative physical picture of how the dynamic Stark spectra depend on the experimental parameters. In order to provide more physical insight to the problem, the theory of Javan is elucidated in Section II of this paper by transforming his expressions into new forms for which the terms can be deduced from simple physical considerations by using a modified energy-level diagram. The relations between a much more complex real system and Javan's simple three-level model are also elucidated in Section II.

The theoretical spectra of high-power 496-μm CH_3F lasers are presented in Section III. This optically pumped FIR laser, due to its simplicity and scalability to very high power, has gained much importance since its invention in 1970 [5]. Currently, megawatt-level pulsed CH_3F lasers are being actively developed at several laboratories to provide a source for Thomson scattering measurement of the ion temperature in Tokamak plasmas [7]. For this application, it is desirable that the spectral width of the laser output be much less than 100 MHz. Experimentally, it has been found that although the highest laser output power can be provided by a "superradiant" CH_3F laser, the total spectral width of such a laser is usually 400–700 MHz wide [8], [9]. While a solution to this problem seems to have been found in oscillator-amplifier combinations [7], a satisfactory explanation of the broad "superradiant" spectrum has hitherto been lacking. The calculated gain spectra we present here are in semiquantitative agreement with experimental observations and show that much of the spectral features of a "superradiant" CH_3F laser can be accounted for by the dynamic Stark effect. From these calculations, we also obtain some guidelines for designing a narrow-band high-power CH_3F laser.

II. Theory

A simplified energy-level diagram for an optically pumped FIR laser is shown in Fig. 1. A pump laser at a frequency ω_p is used to excite the molecules from level i to level j and a tunable probe signal at frequency ω is used to detect the gain or loss near the $j \rightarrow l$ transition. We assume that the system is under steady-state (or quasi-steady-state) pumping and attains certain steady-state vibrational, rotational, and translational temperatures. All perturbations caused by the pump radiation relax toward the steady-state equilibrium at a relaxation rate τ^{-1} where τ is usually the rotational lifetime of the molecules. In the relaxation process, some of the excited molecules will cross over to levels other than the three levels in question. However, we assume that this loss of population from the three-level system is always balanced by a counterflow of molecules from some other levels into the three-level system

Manuscript received June 9, 1977; revised August 9, 1977.
The author is with Bell Laboratories, Holmdel, NJ 07733.

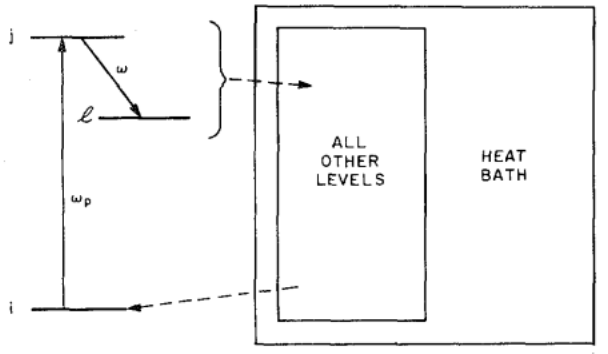

Fig. 1. Basic energy-level diagram of an optically pumped three-level laser. Dashed arrows indicate population flows (assumed to be balanced at all times) to and from other energy levels of the same molecule. Entire molecular gas is assumed to be in thermal equilibrium with a heat bath through collisions.

(primarily due to the refilling of the lowest level i) such that the total population of the three-level system is conserved. We further assume that the probe beam is directed along the x axis, while the pump radiation is linearly polarized along the z axis. In the absence of an external field, each of the molecular energy levels consists of $2J+1$ M sublevels which are degenerate. The transitions between levels i and j and between levels j and l are superpositions of transitions between different M sublevels of these levels. In the following discussions, we shall consider first the elementary transitions of the type $i(M) \rightarrow j(M')$ and $j(M') \rightarrow l(M'')$ among individual M sublevels. We shall use N_i to denote the population density for the level i, and n_i to denote the population density for a sublevel thereof. We assume that the gas pressure is such that all transitions in question are homogeneously broadened.

For a homogeneously broadened line, the power absorbed at ω_p by a pair of sublevels is given by

$$P = (n_{i0} - n_{j0}) \frac{2\tau |y|^2 \hbar \omega_p}{1 + 4\Gamma^2 \tau^2} \tag{1}$$

where

$$y = \mu_{ij}(M, M') E_p / 2\hbar$$

and

$$\Gamma = [(\omega_p - \omega_{ij})^2 + 4|y|^2]^{1/2}/2$$

n_{i0} and n_{j0} being the equilibrium population of the $i(M)$ and $j(M')$ sublevels, respectively, $\mu_{ij}(M, M')$ being the transition dipole moment, and E_p being the strength of the pump field.

The energy of a pump photon may be greater or smaller than the energy separation between levels i and j. In rate equation analysis, this difference is either ignored or assumed to be taken up by collision partners and one obtains the change of population for the $j(M')$ sublevel as

$$\Delta n_j = P/(\hbar\omega_p) = 2(n_{i0} - n_{j0})|y|^2 \tau^2 (1 + 4\Gamma^2\tau^2)^{-1}. \tag{2}$$

This leads to a small signal gain (in the rate equation approximation) near the $j(M') \rightarrow l(M'')$ transition given by

$$\gamma(\omega, M', M'') = \frac{4\pi\omega\tau}{\hbar c} \mu_{jl}^2(M', M'')(\Delta n_j + n_{j0} - n_{l0}) \frac{1}{1 + (\omega - \omega_{jl})^2 \tau^2}. \tag{3}$$

Javan's semiclassical theory of a three-level maser leads, on the other hand, to a much more complex expression for $\gamma(\omega)$. It can be expressed as

$$\gamma(\omega, M', M'') = \frac{8\pi}{c|E|^2} (P_e - P_a) \tag{4}$$

where E is the strength of the probing field (assumed to be weak), and P_e and P_a were given by Javan as

$$P_e = (n_{i0} - n_{l0})\hbar\omega |x|^2 |y|^2 \tau \Gamma^{-2} \cdot \left\{ \frac{1}{2[1 + (\Omega + \Gamma)^2\tau^2]} + \frac{1}{2[1 + (\Omega - \Gamma)^2\tau^2]} - \frac{1 + (1 + 2\Gamma^2\tau^2)(\Omega^2 - \Gamma^2)\tau^2}{(1 + 4\Gamma^2\tau^2)[1 + (\Omega + \Gamma)^2\tau^2][1 + (\Omega - \Gamma)^2\tau^2]} \right\} \tag{4a}$$

$$P_a = (n_{l0} - n_{j0})\hbar\omega |x|^2 \tau (4\Gamma^2)^{-1} \cdot \left\{ \frac{[2\Gamma + (\omega_p - \omega_{ij})]^2}{2[1 + (\Omega + \Gamma)^2\tau^2]} + \frac{[2\Gamma - (\omega_p - \omega_{ij})]^2}{2[1 + (\Omega - \Gamma)^2\tau^2]} + \frac{4|y|^2 [1 + (1 + 2\Gamma^2\tau^2)(\Omega^2 - \Gamma^2)\tau^2]}{(1 + 4\Gamma^2\tau^2)[1 + (\Omega + \Gamma)^2\tau^2][1 + (\Omega - \Gamma)^2\tau^2]} \right\} \tag{4b}$$

with

$$x = \mu_{jl}(M', M'')E/2\hbar$$

and

$$\Omega = (\omega - \omega_{jl}) - \tfrac{1}{2}(\omega_p - \omega_{ij}). \tag{4c}$$

For consistency, we assume that Γ always has the same sign as $(\omega_p - \omega_{ij})$.

It is apparent from the denominators in (4a) and (4b) that the gain or loss occurs primarily near $\Omega \pm \Gamma = 0$, i.e., when

$$\omega = \omega' = \omega_{jl} - \Gamma + \tfrac{1}{2}(\omega_p - \omega_{ij}) = \omega_{jl} - \delta' \tag{5a}$$

and when

$$\omega = \omega'' = \omega_{jl} + \Gamma + \tfrac{1}{2}(\omega_p - \omega_{ij}) = \omega_{jl} + \delta''. \tag{5b}$$

The quantities δ' and δ'' represent the amounts of downward and upward frequency shifts of the two dynamic Stark components [10] from the unperturbed transition and are more explicitly given by

$$\delta' = [\tfrac{1}{4}(\omega_p - \omega_{ij})^2 + |y|^2]^{1/2} - \tfrac{1}{2}(\omega_p - \omega_{ij}) \tag{6a}$$

and

$$\delta'' = [\tfrac{1}{4}(\omega_p - \omega_{ij})^2 + |y|^2]^{1/2} + \tfrac{1}{2}(\omega_p - \omega_{ij}) = \delta' + (\omega_p - \omega_{ij}). \tag{6b}$$

Notice that δ', δ'', and $(\omega_p - \omega_{ij})$ are always of the same sign.

For resonance pumping, $\omega_p = \omega_{ij}$ and we have $\delta' = \delta'' = |y|$. This symmetrical splitting of the $j \to l$ transition is known as the resonance modulation splitting [1]. The population on the j level appears to be modulated by the periodic upward and downward transitions of the molecules between levels j and i at a frequency given by $|y|$, which is also known as the Rabi frequency.

For off-resonance pumping and infinitesimal pump power, i.e., when $\omega_p - \omega_{ij} \neq 0$, and $y \to 0$, we have $\delta' \to 0$ and $\delta'' \to \omega_p - \omega_{ij}$. This means that ω' is unshifted while ω'' shows a Stokes shift from the real transition frequency ω_{jl}; suggesting that the ω' component is primarily due to the ordinary single-photon transition while the ω'' component is primarily due to a Raman-type transition.

As the pump intensity is increased, the ω' and ω'' components shift further away from each other, each by an amount given by δ'. For small values of $|y|$ such that $(\omega_p - \omega_{ij}) >> |y|$, δ' is given approximately by

$$\delta' \approx |y|^2/(\omega_p - \omega_{ij}). \tag{7}$$

To gain further insight into the properties of ω' and ω'' components, it is necessary to put (4) into a much more revealing form. This we have succeeded in doing after rather extensive algebraic manipulation. The following is the result:

$$\gamma(\omega, M', M'') = \frac{4\pi\omega\tau}{\hbar c}\,\mu_{jl}^2(M', M'')\,\{RT + VT + IT\} \tag{8}$$

where

$$RT = \left(\frac{1}{2}\Delta n_j + n_{j0} - n_{l0}\right)\left[\frac{\delta''}{\delta' + \delta''}\,\frac{1}{1 + (\omega - \omega')^2\tau^2} + \frac{\delta'}{\delta' + \delta''}\,\frac{1}{1 + (\omega - \omega'')^2\tau^2}\right] \tag{8a}$$

the ω' and ω'' components. As will become clear from following discussions, the RT term which contains the thermal population difference $n_{j0} - n_{l0}$ is associated with real populations. The VT term, on the other hand, is associated with virtual populations. The IT term arises from the interference between RT and VT terms.

With off-resonance pumping and infinitesimal pump power, (8) reduces to

$$\gamma(\omega, M', M'') \approx \frac{4\pi\omega\tau}{\hbar c}\,\mu_{jl}^2(M', M'')\left\{\left(\frac{1}{2}\Delta n_j + n_{j0} - n_{l0}\right)\cdot\frac{1}{1 + (\omega - \omega')^2\tau^2} + \frac{1}{2}\Delta n_j\,\frac{1}{1 + (\omega - \omega'')^2\tau^2}\right\}. \tag{9}$$

This expression is almost the same as (3) except that in (9) one-half of the Δn_j contribution is shifted to the Stokes frequency ω''. This means that only one-half of Δn_j is real in nature and the other half is virtual.

For finite pump power, both ω' and ω'' components are present in both RT and VT terms. However, the ω' component always has the greater weight $\delta''/(\delta' + \delta'')$ in the RT term, whereas, the ω'' component is always the dominant component in the VT term. The weights of the two components are complementary to each other in both RT and VT terms.

In the IT term, both the ω' component and the ω'' component have a zero integrated strength. The net contribution of the IT term is a distortion of the lineshape near ω' and ω''. The fact that the IT term is an interference term can be brought out more clearly by regrouping the terms in (8) into the following form:

$$\gamma(\omega, M', M'') = \frac{4\pi\omega\tau}{\hbar c}\,\mu_{jl}^2(M', M'')\left\{(n_{j0} - n_{l0})\left[\frac{\delta''}{\delta' + \delta''}\,\frac{1}{1 + (\omega - \omega')^2\tau^2} + \frac{\delta'}{\delta' + \delta''}\,\frac{1}{1 + (\omega - \omega'')^2\tau^2}\right] + \frac{1}{2}\Delta n_j\,\frac{[1 + (\omega - \omega')^2\tau^2] + [1 + (\omega - \omega'')^2\tau^2] + [1 + (\omega - \omega')(\omega'' - \omega)\tau^2]}{[1 + (\omega - \omega')^2\tau^2]\,[1 + (\omega - \omega'')^2\tau^2]}\right\}. \tag{10}$$

$$VT = \frac{1}{2}\Delta n_j\left[\frac{\delta'}{\delta' + \delta''}\,\frac{1}{1 + (\omega - \omega')^2\tau^2} + \frac{\delta''}{\delta' + \delta''}\,\frac{1}{1 + (\omega - \omega'')^2\tau^2}\right] \tag{8b}$$

$$IT = \frac{1}{2}\Delta n_j\left[\frac{\omega - \omega'}{\omega'' - \omega'}\,\frac{1}{1 + (\omega - \omega')^2\tau^2} + \frac{\omega - \omega''}{\omega' - \omega''}\,\frac{1}{1 + (\omega - \omega'')^2\tau^2}\right] \tag{8c}$$

with Δn_j given by (2), ω' and ω'' given by (5a) and (5b), and δ' and δ'' given by (6a) and (6b). Notice that $\delta' + \delta'' = \omega'' - \omega' = 2\Gamma$ is the total distance between the nominal positions of

Here, the last factor in the numerator of the last term corresponds to the IT term.

In most optically pumped FIR lasers, the thermal population difference $(n_{j0} - n_{l0})$ is negligible. Whenever this is true the ω' and ω'' components are always of the same strength. The shapes of the lines are, however, distorted from a Lorentzian shape by the interference term, and the actual peaks of the two components are shifted somewhat closer together from the nominal positions ω' and ω''.

A finite value of $(n_{j0} - n_{l0})$, normally negative, leads to thermal absorption occurring primarily at ω'. The laser gain at ω' is reduced relative to the gain at ω'' by the presence of this thermal absorption, sometimes to the point that the ω' component becomes absorbing while the ω'' component is still showing gain (predominantly of Raman type) [4].

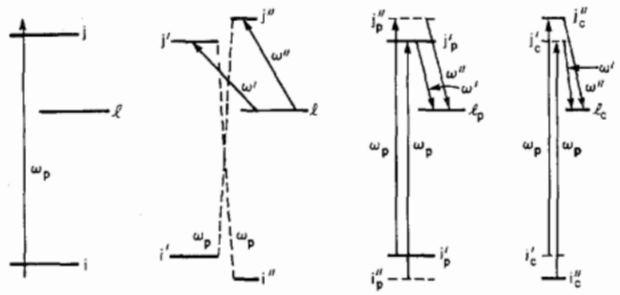

Fig. 2. Effect of dynamic Stark effect on the energy levels. (a) Original energy levels. (b) Sidebands generated by the pump field and the splitting and shifting of the $l \rightarrow j$ absorption line. (c) Principal subsystem [with a weight of $\delta''/(\delta' + \delta'')$], showing the real (solid lines) and virtual (broken lines) levels and the transitions among them. (d) Complementary subsystem.

To obtain an even clearer physical picture of the dynamic Stark effect, it is instructive to deduce (8a) and (8b) from an energy-level diagram. Depicted in Fig. 2(a) are the three unperturbed energy levels and the pump frequency which is generally off resonant. In general, the action of the pump field leads to weak sideband energy levels which are separated from the main energy levels by ω_p as shown in Fig. 2(b). Since the two sideband levels i'' and j'' shown in Fig. 2(b) are close in energy to the j and i levels, they are resonantly enhanced and assume the properties of the latter levels. The thermal population on level j is divided up between sublevels j' and j'' according to their relative weights. The relative weights and frequency shifts of j' and j'' levels are such that the center of mass of the two sublevels remains at the original position of the j level. These considerations lead immediately to the terms containing $(n_{j0} - n_{l0})$ in (8a) and (10). The level i is split in the same way as the level j.

For further discussions, it is convenient to artificially split the energy-level system into a principal subsystem of weight $\delta''/(\delta' + \delta'')$ as shown in Fig. 2(c) and a complementary subsystem of weight $\delta'/(\delta' + \delta'')$ as shown in Fig. 2(d). Now consider a molecule in the principal subsystem. According to the semiclassical model adopted by Javan [6], when a molecule suffers a collision, it is removed from the interaction with the pump field and then immediately reentered into the system of three real energy levels according to the Boltzmann distribution. Between collisions each molecule is a lossless oscillator. It is well known that when a lossless classical oscillator is suddenly subjected to an off-resonant driving force, its response will consist of equal amplitudes of excitation at both the natural frequency of the oscillator and the driving frequency of the pump source. Semiclassically, this means that if a molecule is entered into level i'_p, then it has the equal probability of being excited into either the real level j'_p (represented by a solid line) or the virtual level j''_p (represented by a broken line). The same considerations apply to the complementary subsystem shown in Fig. 2(d). Of the four resulting emission transitions shown in Fig. 2(c) and (d) the ones with a real intermediate level lead naturally to the terms associated with $\frac{1}{2}\ \Delta n_j$ in (8a), and the ones with a virtual intermediate level lead to the terms in (8b). If we combine Fig. 8(c) and (d), we see easily that one-half of the excited population Δn_j leads to gain at ω' and the other half to gain at ω'' as in (10). The interference term cannot be deduced from the energy-level diagrams, but can be easily remembered in the form of (10). We note in passing that since the virtual levels i''_p and i'_c have no thermal population, the pumping action represented by upward arrows in Fig. 2(c) and (d) leads to negative virtual populations (which represent only a mathematical concept) on these levels. It can be shown, however, that the combined population of levels i''_p and $i''_{c'}$ as well as the combined population of levels i''_p and $i''_{c'}$ are always positive.

In the case of optically pumped CH_3F, several $Q(12, K)$ transitions are affected by the same pump field. The principal subsystems for $K = 1$ to 3 transitions are illustrated in Fig. 3. The optical gain experienced by a probe beam is the sum of contributions from these and other K transitions.

As we have stated in the outset, the above discussions pertain to a pair of transition among specific M sublevels in the i, j, and l energy levels. To obtain the complete result, we must sum over all possible values of M, M', and M''. Relevant dipole matrix elements for these transitions can be found, e.g., in Townes and Schawlow [10]. The final result has quite complex dependences on the values of (J, K), (J', K'), and (J'', K''). In order to make further general discussion of $\gamma(\omega)$ possible, we shall use a rather simplified classical model. We assume that the molecules exist in three groups, with the total angular momentum vector J oriented, respectively, along the x, y, and z axes. The corresponding molecular densities are given by $n_{kox} = n_{koy} = n_{koz} = N_k/3$, where $k = i, j$, or l. These nine population components give rise to nine separate contributions to the total laser gain, which we can write as $\gamma(\omega) = \Sigma_{k,w}\ \gamma_{kow}(\omega)$. Each of the γ_{kow} terms contains only one n_{kow} component and its appropriate transition dipole moment. The latter depends on whether the probe beam is z polarized or y polarized. For generality, we shall denote by u the direction of polarization of the probe beam. The pump beam is already assumed to be z polarized. The appropriate dipole moment components for n_{iow} are μ_{ijz} and μ_{jlu}, those for n_{jow} are μ_{jiz} and μ_{jlu}, and those for n_{low} are μ_{jiz} and μ_{lju}. The values of these dipole moment components depend on whether the subscript w stands for x, y, or z, and many of them are identically zero. For instance, for molecules in the n_{iox} group, if the pump transition follows the selection rule $|\Delta J| = 1$, then $\mu_{ijx} = 0$, while $\mu^2_{ijy} = \mu^2_{ijz} = \frac{1}{2}\ \mu^2_{ij}$. Whereas, if the pump transition follows the selection rule $\Delta J = 0$, then $\mu_{ijy} = \mu_{ijz} = 0$, while $\mu_{ijx} = \mu_{ij}$. Corresponding relations for other n_{kow} components can be obtained from these relations by permutating the subscripts. The same pattern also applies to the $j \rightarrow l$ transition. It should be kept in mind that $\mu^2_{ij} = (g_i/g_j)\mu^2_{ji}$, where g_k denotes the degeneracy number of the level k.

The gain resulting from these calculations is different for z and y probe polarizations. For Q-branch pump transition, the gain is mainly y polarized, while for P or R-branch pump transition, the gain is mainly z polarized. The degree of gain polarization obtained from this simplified model is, however, not very accurate. For high J values and low pump field, a better estimate of the polarization pattern of the gain can be obtained by assuming an isotropic distribution of J, and integrate the contributions from various molecular orientations over all

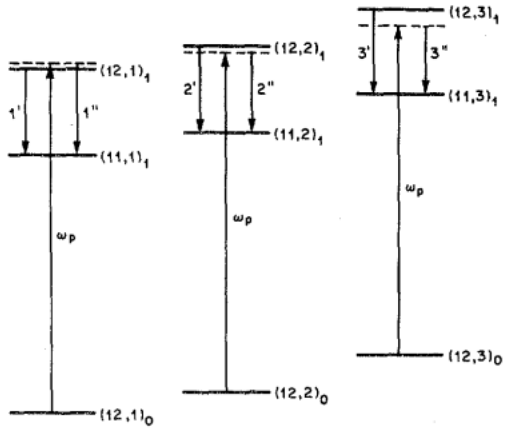

Fig. 3. Principal subsystems for $K = 1$, 2, and 3 manifolds in a CH_3F laser. Notations $(12, 2)_1$, etc., stand for $J = 12$, $K = 2$, $n(\nu_3) = 1$, etc. The notations 2′ and 2″, etc., stand for $\omega'(K = 2)$, $\omega''(K = 2)$, etc.

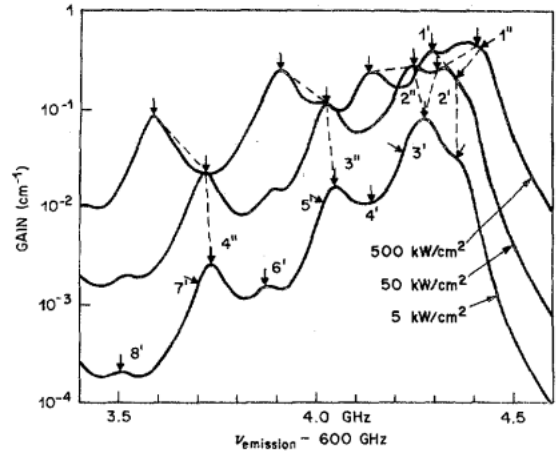

Fig. 4. Calculated gain spectra for a CH_3F laser for pump intensities of 5, 50, and 500 kW/cm^2. Short arrows indicate the positions of various components and the dashed lines indicate the shift of some of these components with the pump intensity. Positions of some components are not indicated for higher curves to avoid cluttering of the figure.

solid angles [11]. The most rigorous result is of course obtained by summing over all possible values of M, M', and M''. Due to the dependence of dipole moments on M, M', and M'', various M components in the gain spectrum show different amounts of dynamic Stark shifts and exhibit different strengths. As a result, the gain lines near ω' and ω'' are usually asymmetrically broadened and exhibit substructures due to these M subcomponents [12].

III. Numerical Results

The gain spectrum of an optically pumped CH_3F laser has been studied numerically using the expressions given in the preceding section. Contributions from $K = 1$ to 11 components are all included. (The $K = 0$ component is not allowed for the pump transition, while the $K = 12$ component is not allowed for the emission transition.) The laser gain was calculated for a y-polarized probe beam, with the polarization properties treated in the simplified classical approximation discussed above. Since in the CH_3F laser $(N_i - N_j) < 10^{-3}(N_i - N_j)$, we have neglected the effect of $N_I - N_j$ in the calculation. The pump laser was assumed to be tuned to the center of the $P(20)$ line of the CO_2 laser at 9.55 μm. The unperturbed positions of the $Q(12, K)$ transitions in CH_3F were calculated according to the formula

$$Q(12,K) = P(20)_{CO_2} - 69.14 + 27.33\,K^2 + 0.145\,K^4 \text{ (MHz)},$$

whereas the positions of the unperturbed emission transitions were calculated according to the formula

$$\nu_e(11,K) = 604,350 - 13.2\,K^2 \text{ (MHz)}.$$

The coefficients are obtained from [5], [13]–[15] and represent a compromise in some cases. The CH_3F pressure was assumed to be 2 torr.

The calculated gain spectra for three different pump intensities are shown in Fig. 4. The locations of some of the K components are also identified (peaks within 75 MHz of each other are not resolved). At power densities below 5 kW/cm^2, the $K = 2$ component is always dominant, and a stable, narrow oscillation bandwidth can be expected. At power densities in excess of 50 kW/cm^2, the $K = 2$ components (labeled 2′ and 2″) are strongly saturated and are significantly split by the dynamic Stark effect. In this high-power regime, the spectrum changes considerably with the pump power, and the $K = 1$ and $K = 3$ components become very strong.

The pump power dependences of gain and frequency for various components are plotted in Fig. 5. At 2-torr pressure, the Raman-type (ω'') and single quantum (ω') components are unresolved when they are within ~75 MHz of each other. The broken curves for $K = 1$, 2 and 3 components in Fig. 5 give the apparent peaks of the sum of these components. The curves on the left-hand side of Fig. 5 represent the values of gain at the apparent peaks of various components. Notice that, due to the three-fold symmetry of CH_3F with three identical atoms of spin 1/2, $K = 3$, 6, 9, 12 levels have twice the statistical weight of all other K levels. Consequently, the saturated gain of $K = 3$ components are higher than those of $K = 1$, and 2 components.

We can predict the "superradiant" spectrum of a high power CH_3F laser semiquantitatively with the aid of Fig. 5. According to the study by Herman *et al.* [16], a total gain γL of greater than 20 is necessary to produce an appreciable "superradiant" pulse buildup. In both of the two experimental studies cited for the superradiant CH_3F laser [8], [9], the gain length is approximately 3 m. Hence the threshold value of γ for superradiance can be expected to be greater than 0.067 cm^{-1}. Experimentally, Brown *et al.* [8] deduced a lower bound of γ to be 30 dB/m or 0.069 cm^{-1} for their system. From these considerations, we take $\gamma = 0.07$ cm^{-1} to be the threshold gain for superradiance in these systems. Some uncertainties in this threshold value will not seriously affect our conclusions.

We assume that the rise time of the pump pulse is much longer than the collision time such that a quasi-steady-state prevails at all times during the pump pulse and the above analysis is approximately applicable. As the pump power rises from a very small value to a high peak value, the $K = 2$, $K = 1$, and $K = 3$ components will successively reach the superradiant

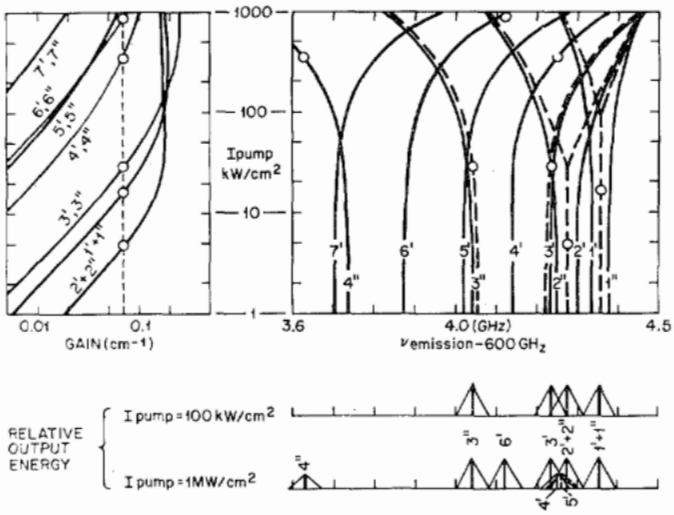

Fig. 5. Dependences of gain and frequency of various spectral components on the pump intensity in a CH_3F laser. Broken curves in the right-hand part of the figure indicate the apparent positions of gain peaks due to the overlapping of ω' and ω'' components. The circles indicate the points at which the gain values of various components reach the superradiant threshold of 0.07 cm^{-1}. Lower part of the figure depicts the expected superradiant spectra at two different pump intensities.

gain (as shown in the left-hand part of Fig. 5) and emit superradiant pulses that are separated both in time and in frequency. The expected locations of emission lines and their probable strengths (proportional to their statistical weights) are shown in the lower part of Fig. 5 for pump powers of 100 kW/cm^2 and 1 MW/cm^2. At 1 MW/cm^2, the 4″ and 6″ subcomponents (i.e., ω'' for $K = 4$ and $K = 6$) are very far removed from the main cluster of emission peaks and might be easily overlooked in Fabry-Perot analyses of the emission spectrum. All the other superradiant components form a cluster centered around 604.2 GHz. The separation between the two extreme peaks ($1' + 1''$ and $3''$) in this main cluster is ~320 MHz and is independent of the peak pump power if the latter is greater than 30 kW/cm^2. This conclusion is in reasonably good agreement with experimental observations.

The presence of a strong far infrared field will also lead to further dynamic Stark splitting and shifting of the energy levels as shown recently by Panock and Temkin [17]. However, since the frequency of a superradiant pulse is determined primarily during the early stage of pulse build up, such an effect is not likely to be important for the strongest component which builds up first. The spectra of other components that build up subsequently can be shifted and smeared by the far infrared field to some extent. Although we have neither taken into account this effect of the far infrared field nor looked into the possible effect of the stronger K components emitting more than one superradiant pulse with different amounts of dynamic Stark shift during a single pump pulse, we believe we have provided a much improved interpretation of the superradiant emission spectrum of a CH_3F laser. Contrary to previous interpretations [8], [9], it is clear that under no circumstances can $K = 4, 5, 6$ components dominate over $K = 1, 2, 3$ components, and that the spacings of peaks in the emission spectrum cannot be correlated with the spacings of unperturbed K components. We also learn from Fig. 5 that in order for the $K = 2$ component to dominate over all other components, so as to obtain a narrow emission spectrum from a given device (with or without feedback), the pump intensity should be kept below ~10 kW/cm^2. The $K = 1$ and 3 components will be difficult to suppress when the peak pump intensity exceeds 100 kW/cm^2.

References

[1] S. H. Autler and C. H. Townes, "Stark effect in rapidly varying fields," *Phys. Rev.*, vol. 100, pp. 703–722, 1955.

[2] A. M. Bonch-Bruevich, N. N. Kostin, V. A. Khodovoi, and V. V. Khromov, "Changes in the atomic absorption spectrum in the field of a light wave, I," *Sov. Phys.–JETP*, vol. 29, pp. 82–85, 1969; P. F. Liao and J. E. Bjorkholm, "Direct observation of atomic energy level shifts in two-photon absorption," *Phys. Rev. Lett.*, vol. 34, pp. 1–4, 1975.

[3] I. M. Beterov and V. P. Chebotaev, "Three-level gas laser," *JETP Lett.*, vol. 9, pp. 127–130, 1969; T. Hansch, R. Keil, A. Schabert, C. H. Schmelzer, and P. Toschek, "Interaction of laser light waves by dynamic Stark splitting," *Z. Phys.*, vol. 226, pp. 293–296, 1969.

[4] T. Y. Chang and J. D. McGee, "Off-resonant infrared laser action in NH_3 and C_2H_4 without population inversion," *Appl. Phys. Lett.*, vol. 29, pp. 725–727, 1976.

[5] T. Y. Chang and T. J. Bridges, "Laser action at 452, 496 and 541 μm in optically pumped CH_3F," *Opt. Commun.*, vol. 1, pp. 423–426, 1970.

[6] A. Javan, "Theory of a three-level maser," *Phys. Rev.*, vol. 107, pp. 1579–1589, 1957.

[7] Z. Drozdowicz, P. Woskoboinikow, K. Isobe, D. R. Cohn, R. J. Temkin, K. J. Button, and J. Waldman, "High power optically pumped far infrared laser systems," *IEEE J. Quantum Electron.*, vol. QE-13, pp. 413–417, June 1977; F. Brown, P. D. Hislop, and J. O. Tarpinian, "A high-power, narrow-linewidth, linearly pumped CH_3F oscillator-amplifier system," *IEEE J. Quantum Electron.*, vol. QE-13, pp. 445–446, June 1977; D. E. Evans, L. E. Sharp, W. A. Peebles, and G. Taylor, "A high-intensity narrow bandwidth pulsed submillimeter laser for plasma diagnostics," *IEEE J. Quantum Electron.*, vol. QE-13, pp. 54–58, June 1977, A. Semet, and N. C. Luhmann, Jr., "High-power narrow-line pulsed 496 μm laser," *Appl. Phys. Lett.*, vol. 28, pp. 659–661, 1976.

[8] F. Brown, S. R. Horman, and A. Palevsky, "Characteristics of a 30-kW-peak, 496-μm, methyl fluoride laser," *Opt. Commun.*, vol. 9, pp. 28–30, 1973; F. Brown, S. Kronheim, and E. Silver, "Tunable far infrared methyl fluoride laser using transverse optical pumping," *Appl. Phys. Lett.*, vol. 25, pp. 394–396, 1974.

[9] D. E. Evans, B. W. James, W. A. Peebles, and L. E. Sharp, "Spectral composition of FIR laser radiation optically excited in methyl fluoride," *Infrared Phys.*, vol. 16, pp. 193–195, 1976.

[10] C. H. Townes and A. L. Schawlow, *Microwave Spectroscopy*. New York: McGraw-Hill, 1955, pp. 273–283, p. 96.

[11] T. Y. Chang, "Optical pumping in gases," in *Nonlinear Infrared Generation*, Y. R. Shen, Ed. Berlin: Springer-Verlag, 1977, pp. 215–272.

[12] N. Skribanowitz, M. J. Kelly, and M. S. Feld, "New laser technique for the identification of molecular transitions," *Phys. Rev.*, vol. A 6, pp. 2302–2311, 1972.

[13] S. M. Freund, G. Duxbury, M. Romheld, J. T. Tiedje, and T. Oka, "Laser Stark spectroscopy in the 10-μm region: The ν_3 bands of CH_3F," *J. Mol. Spectrosc.*, vol. 52, pp. 38–57, 1974.

[14] D. T. Hodges and J. R. Tucker, "Pump absorption and saturation in the CH_3F 496-μm laser," *Appl. Phys. Lett.*, vol. 27, pp. 667–669, 1975.

[15] G. Kramer and C. O. Weiss, "Frequencies of some optically pumped submillimeter laser lines," *Appl. Phys.*, vol. 10, pp. 187–188, 1976.

[16] I. P. Herman, J. C. MacGillivray, N. Skribanowitz, and M. S. Feld, "Self-induced emission in optically pumped HF gas: The rise and fall of the superradiant state," in *Laser Spectroscopy*, R. G. Brewer and A. Mooradian, Eds. New York: Plenum, 1974, pp. 379–412.

[17] R. L. Panock and R. J. Temkin, "Interaction of two laser fields with a three-level molecular system," *IEEE J. Quantum Electron.*, vol. QE-13, pp. 425–434, June 1977.